

Hypernovae, Black-Hole-Forming Supernovae, and First Stars

K. Nomoto, N. Tominaga, H. Umeda, K. Maeda, T. Ohkubo, J. Deng,
P.A. Mazzali

*Department of Astronomy and Research Center for the Early Universe,
University of Tokyo, Bunkyo-ku, Tokyo 113-0033, Japan*
INAF-Osservatorio Astronomico, Via Tiepolo, 11, 34131 Trieste, Italy

Abstract.

Recent studies of core-collapse supernovae have revealed the existence of two distinct classes of massive supernovae (SNe): 1) very energetic SNe (Hypernovae), whose kinetic energy (KE) exceeds 10^{52} erg, about 10 times the KE of normal core-collapse SNe, and 2) very faint and low energy SNe ($E \lesssim 0.5 \times 10^{51}$ erg; Faint supernovae). These two classes of supernovae are likely to be "black-hole-forming" supernovae with rotating or non-rotating black holes. We compare their nucleosynthesis yields with the abundances of extremely metal-poor (EMP) stars to identify the Pop III (or first) supernovae. We show that the EMP stars, especially the C-rich type, are likely to be enriched by black-hole-forming supernovae.

1. Introduction and Summary

Stars more massive than $\sim 25 M_{\odot}$ form a black hole at the end of their evolution. Stars with non-rotating black holes are likely to collapse "quietly" ejecting a small amount of heavy elements (Faint supernovae). In contrast, stars with rotating black holes are likely to give rise to very energetic supernovae (Hypernovae). We present distinct nucleosynthesis features of these two classes of "black-hole-forming" supernovae. Nucleosynthesis in Hypernovae is characterized by larger abundance ratios (Zn,Co,V,Ti)/Fe and smaller (Mn,Cr)/Fe than normal supernovae, which can explain the observed trend of these ratios in extremely metal-poor stars. Nucleosynthesis in Faint supernovae is characterized by a large amount of fall-back. We show that the abundance pattern of the recently discovered most Fe-poor star, HE0107-5240, and other extremely metal-poor stars are in good accord with those of black-hole-forming supernovae, but not pair-instability supernovae. This suggests that black-hole-forming supernovae made important contributions to the early Galactic (and cosmic) chemical evolution. Finally we discuss the nature of First (Pop III) Stars.

2. Hypernovae and Faint Supernovae

Type Ic Hypernovae 1998bw and 2003dh were clearly linked to the Gamma-Ray Bursts GRB 980425 (Galama et al. 1998) and GRB 030329 (Stanek et al. 2003; Hjorth et al. 2003), thus establishing the connection between long GRBs

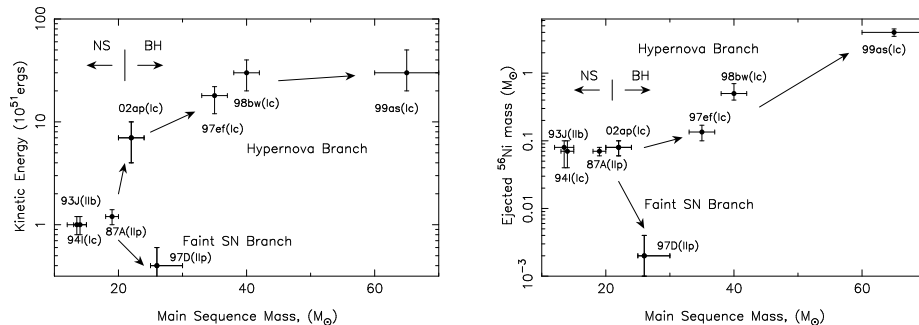


Figure 1. The explosion energy and the ejected ^{56}Ni mass as a function of the main sequence mass of the progenitors for several supernovae/hypernovae (Nomoto et al. 2003).

and core-collapse supernovae (SNe). SNe 1998bw and 2003dh were exceptional for SNe Ic: they were as luminous at peak as a SN Ia, indicating that they synthesized $0.3 - 0.5 M_{\odot}$ of ^{56}Ni , and their kinetic energy (KE) were estimated as $E_{51} = E/10^{51} \text{ erg} \sim 30$ (Iwamoto, Mazzali, Nomoto, et al. 1998; Woosley, Eastman, & Schmidt 1999; Nakamura et al. 2001a; Mazzali et al. 2003).

Other “hypernovae” have been recognized, such as SN 1997ef (Iwamoto et al. 2000; Mazzali, Iwamoto, & Nomoto 2000), SN 1999as (Knop et al. 1999; Hatano et al. 2001), and SN 2002ap (Mazzali et al. 2002). These hypernovae span a wide range of properties, although they all appear to be highly energetic compared to normal core-collapse SNe. The mass estimates, obtained from fitting the optical light curves and spectra, place hypernovae at the high-mass end of SN progenitors.

In contrast, SNe II 1997D and 1999br were very faint SNe with very low KE (Turatto et al. 1998; Hamuy 2003; Zampieri et al. 2003). In the diagram that shows E and the mass of ^{56}Ni ejected $M(^{56}\text{Ni})$ as a function of the main-sequence mass M_{ms} of the progenitor star (Figure 1), therefore, we propose that SNe from stars with $M_{\text{ms}} \gtrsim 20\text{--}25 M_{\odot}$ have different E and $M(^{56}\text{Ni})$, with a bright, energetic “hypernova branch” at one extreme and a faint, low-energy SN branch at the other (Nomoto et al. 2003). For the faint SNe, the explosion energy was so small that most ^{56}Ni fell back onto the compact remnant. Thus the faint SN branch may become a “failed” SN branch at larger M_{ms} . Between the two branches, there may be a variety of SNe (Hamuy 2003).

This trend might be interpreted as follows. Stars with $M_{\text{ms}} \lesssim 20\text{--}25 M_{\odot}$ form a neutron star, producing $\sim 0.08 \pm 0.03 M_{\odot}$ ^{56}Ni as in SNe 1993J, 1994I, and 1987A. Stars with $M_{\text{ms}} \gtrsim 20\text{--}25 M_{\odot}$ form a black hole; whether they become hypernovae or faint SNe may depend on the angular momentum in the collapsing core, which in turn depends on the stellar winds, metallicity, magnetic fields, and binarity. Hypernovae might have rapidly rotating cores owing possibly to the spiraling-in of a companion star in a binary system.

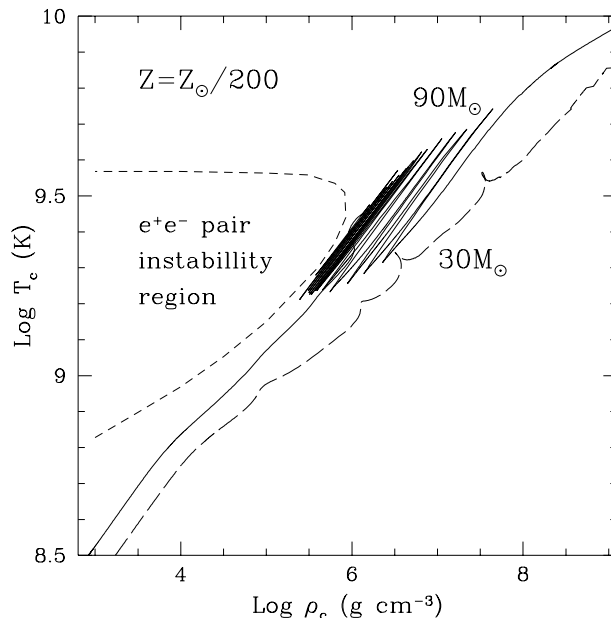


Figure 2. Evolution of the central density and temperature for the 30 and 90 M_{\odot} models (Umeda & Nomoto 2004)

3. Synthesis of ^{56}Ni in $\sim 100M_{\odot}$ Stars

The light curve modeling of the unusually bright hypernova SN1999as suggests that the progenitor is a core-collapse supernova and the ejected ^{56}Ni mass is as large as $\sim 3 - 4M_{\odot}$. Motivated by SN 1990as, Umeda & Nomoto (2004) have investigated how much ^{56}Ni can be synthesized in core-collapse massive supernovae.

The evolutions of several very massive stars with initial masses of $M \leq 100M_{\odot}$ and low metallicity ($Z = Z_{\odot}/200$) have been calculated from the main-sequence to “hypernova” explosions. The synthesized ^{56}Ni mass increases with the increasing explosion energy and the progenitor mass. Umeda & Nomoto (2004) found that for the explosion energy of 3×10^{52} ergs, for example, the ^{56}Ni mass of up to 2.2, 2.3, 5.0, and $6.6 M_{\odot}$ can be produced for the progenitors with masses of 30, 50, 80 and $100 M_{\odot}$, that are sufficiently large to explain SN 1999as.

Figure 2 shows the evolution of the central density and temperature for the 30 and $90M_{\odot}$ models. More massive stars have larger specific entropy at the center, thus having higher temperature for the same density. For $90M_{\odot}$, the evolutionary track is very close to (but outside of) the “ $e^{-}e^{+}$ pair-instability region” of $\Gamma < 4/3$ where Γ denotes the adiabatic index. The evolution of the central temperature and density is significantly different between the 30 and $90M_{\odot}$ models during Si-burning at $T_9 = T/10^9\text{K} = 2.5 - 4$. The central temperature and density of the $90M_{\odot}$ model oscillate several times. This is because in such massive stars radiation pressure is so dominant that Γ is close to $4/3$, and thus the inner core of the stars easily expands with the nuclear energy released by Si-burning. Once it expands, the temperature drops suddenly, the

central Si-burning stops, and the stellar core turns into shrink. Since only small amount of Si is burnt for each cycle, this pulsations occur many times.

Umeda & Nomoto (2004) found from the study of $80\text{--}100M_{\odot}$ stars that the number of the oscillations depends on the convective parameter f_k : larger f_k increases the number of the oscillation. This is because for a larger f_k fresh Si is mixed more efficiently into the center, which increase the lifetime of this stage. The situation is similar to the breathing pulse phase at the end of He-burning, while the variation of the temperature and density is much larger in Si burning than in the breathing pulse phase. The amplitude of the temperature and density variation is larger for more massive stars, which suggests more and more drastic oscillations would occur for larger mass stars.

4. Nucleosynthesis in Hypernovae

In core-collapse supernovae/hypernovae, stellar material undergoes shock heating and subsequent explosive nucleosynthesis. Iron-peak elements are produced in two distinct regions, which are characterized by the peak temperature, T_{peak} , of the shocked material. For $T_{\text{peak}} > 5 \times 10^9 \text{K}$, material undergoes complete Si burning whose products include Co, Zn, V, and some Cr after radioactive decays. For $4 \times 10^9 \text{K} < T_{\text{peak}} < 5 \times 10^9 \text{K}$, incomplete Si burning takes place and its after decay products include Cr and Mn (Nakamura et al. 1999).

4.1. Supernovae vs. Hypernovae

The right panel of Figure 3 shows the composition in the ejecta of a $25 M_{\odot}$ hypernova model ($E_{51} = 10$). The nucleosynthesis in a normal $25 M_{\odot}$ SN model ($E_{51} = 1$) is also shown for comparison in the left panel of Figure 3 (Umeda & Nomoto 2002).

We note the following characteristics of nucleosynthesis with very large explosion energies (Nakamura et al. 2001b; Nomoto et al. 2001; Umeda & Nomoto 2005):

(1) Both complete and incomplete Si-burning regions shift outward in mass compared with normal supernovae, so that the mass ratio between the complete and incomplete Si-burning regions becomes larger. As a result, higher energy explosions tend to produce larger $[(\text{Zn}, \text{Co}, \text{V})/\text{Fe}]$ and smaller $[(\text{Mn}, \text{Cr})/\text{Fe}]$, which can explain the trend observed in very metal-poor stars (Umeda & Nomoto 2005).

(2) In the complete Si-burning region of hypernovae, elements produced by α -rich freezeout are enhanced. Hence, elements synthesized through capturing of α -particles, such as ^{44}Ti , ^{48}Cr , and ^{64}Ge (decaying into ^{44}Ca , ^{48}Ti , and ^{64}Zn , respectively) are more abundant.

(3) Oxygen burning takes place in more extended regions for the larger KE. Then more O, C, Al are burned to produce a larger amount of burning products such as Si, S, and Ar. Therefore, hypernova nucleosynthesis is characterized by large abundance ratios of $[\text{Si}, \text{S}/\text{O}]$, which can explain the abundance feature of M82 (Umeda et al. 2002).

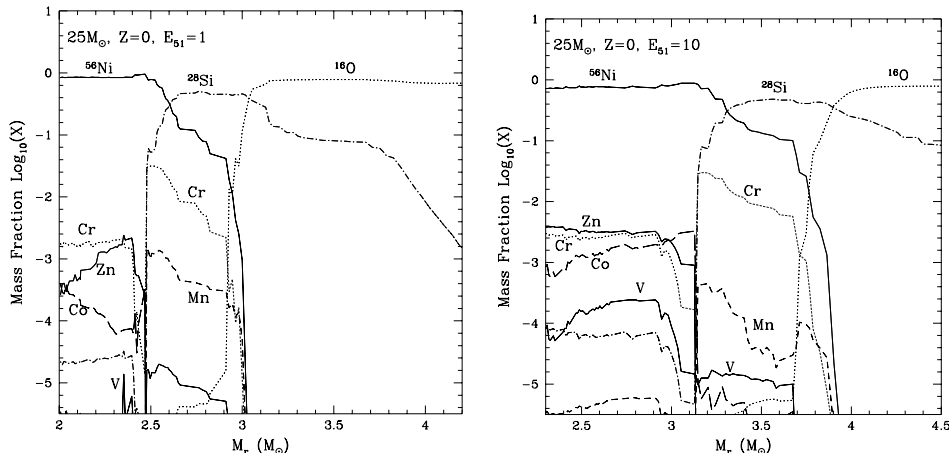


Figure 3. Abundance distribution against the enclosed mass M_r after the explosion of Pop III $25 M_{\odot}$ stars with $E_{51} = 1$ (left) and $E_{51} = 10$ (right) (Umeda & Nomoto 2002).

4.2. Hypernovae and Zn, Co, Mn, Cr

Hypernova nucleosynthesis may have made an important contribution to Galactic chemical evolution. In the early galactic epoch when the galaxy was not yet chemically well-mixed, $[\text{Fe}/\text{H}]$ may well be determined by mostly a single SN event (Audouze & Silk 1995). The formation of metal-poor stars is supposed to be driven by a supernova shock, so that $[\text{Fe}/\text{H}]$ is determined by the ejected Fe mass and the amount of circumstellar hydrogen swept-up by the shock wave (Ryan, Norris, & Beers 1996). Then, hypernovae with larger E are likely to induce the formation of stars with smaller $[\text{Fe}/\text{H}]$, because the mass of interstellar hydrogen swept up by a hypernova is roughly proportional to E (Ryan et al. 1996; Shigeyama & Tsujimoto 1998) and the ratio of the ejected iron mass to E is smaller for hypernovae than for normal supernovae.

In the observed abundances of halo stars, there are significant differences between the abundance patterns in the iron-peak elements below and above $[\text{Fe}/\text{H}] \sim -2.5$ - -3 .

(1) For $[\text{Fe}/\text{H}] \lesssim -2.5$, the mean values of $[\text{Cr}/\text{Fe}]$ and $[\text{Mn}/\text{Fe}]$ decrease toward smaller metallicity, while $[\text{Co}/\text{Fe}]$ increases (McWilliam et al. 1995; Ryan et al. 1996).

(2) $[\text{Zn}/\text{Fe}] \sim 0$ for $[\text{Fe}/\text{H}] \simeq -3$ to 0 (Snedden, Gratton, & Crocker 1991), while at $[\text{Fe}/\text{H}] < -3.3$, $[\text{Zn}/\text{Fe}]$ increases toward smaller metallicity (Cayrel et al. 2004).

The larger $[(\text{Zn}, \text{Co})/\text{Fe}]$ and smaller $[(\text{Mn}, \text{Cr})/\text{Fe}]$ in the supernova ejecta can be realized if the mass ratio between the complete Si burning region and the incomplete Si burning region is larger, or equivalently if deep material from the complete Si-burning region is ejected by mixing or aspherical effects. This can be realized if (1) the mass cut between the ejecta and the compact remnant is located at smaller M_r (Nakamura et al. 1999), (2) E is larger to move the outer edge of the complete Si burning region to larger M_r (Nakamura et al. 2001b), or (3) asphericity in the explosion is larger.

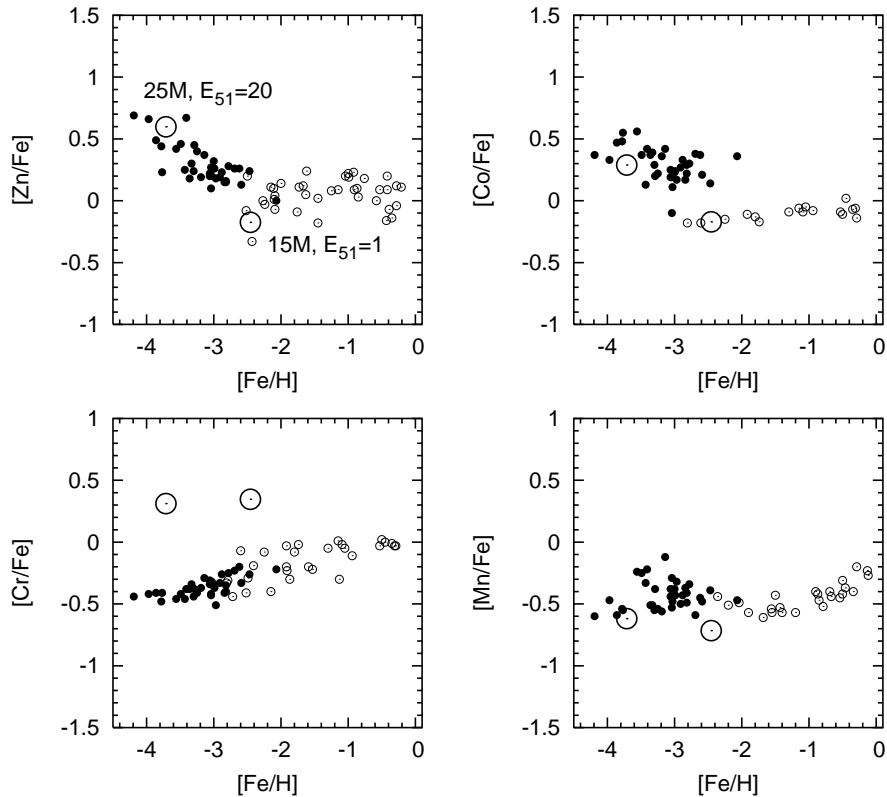


Figure 4. Observed abundance ratios of $[Zn, Co, Cr, Mn/Fe]$ vs $[Fe/H]$ (Cayrel et al. 2004) compared with $(15 M_{\odot}, E_{51} = 1)$ and $(25 M_{\odot}, E_{51}=30)$ models (Tominaga et al. 2005).

Among these possibilities, a large explosion energy E enhances α -rich freeze-out, which results in an increase of the local mass fractions of Zn and Co, while Cr and Mn are not enhanced (Umeda & Nomoto 2002, 2005). Models with $E_{51} = 1$ do not produce sufficiently large $[Zn/Fe]$. To be compatible with the observations of $[Zn/Fe] \sim 0.5$, the explosion energy must be much larger, i.e., $E_{51} \gtrsim 20$ for $M \gtrsim 20 M_{\odot}$, i.e., hypernova-like explosions of massive stars ($M \gtrsim 25 M_{\odot}$) with $E_{51} > 10$ are responsible for the production of Zn.

In the hypernova models, the overproduction of Ni, as found in the simple “deep” mass-cut model, can be avoided (Umeda & Nomoto 2005). Therefore, if hypernovae made significant contributions to the early Galactic chemical evolution, it could explain the large Zn and Co abundances and the small Mn and Cr abundances observed in very metal-poor stars (Fig. 4: Tominaga et al. 2005).

5. Extremely Metal-Poor (EMP) Stars

Recently the most Fe deficient and C-rich low mass star, HE0107-5240, was discovered (Christlieb et al. 2002, 2004). This star has $[Fe/H] = -5.3$ but its mass is as low as $0.8 M_{\odot}$. This would challenge the recent theoretical arguments that

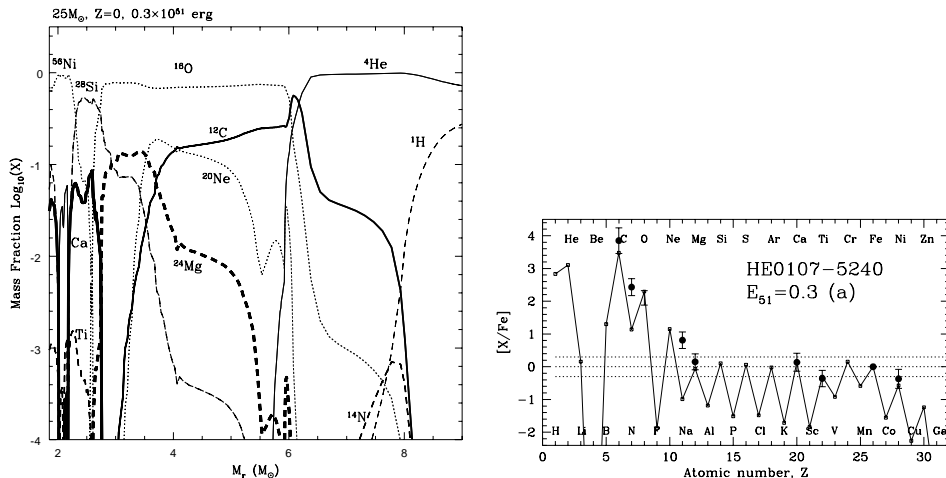


Figure 5. (left) The post-explosion abundance distributions for the $25 M_{\odot}$ model with the explosion energy $E_{51} = 0.3$. (right) Elemental abundances of the C-rich, most Fe deficient star HE0107-5240 (Christlieb et al. 2004: filled circles), compared with a theoretical supernova yield (Umeda & Nomoto 2003, 2005).

the formation of low mass stars, which should survive until today, is suppressed below $[\text{Fe}/\text{H}] = -4$ (Schneider et al. 2002).

The important clue to this problem is the observed abundance pattern of this star. This star is characterized by a very large ratios of $[\text{C}/\text{Fe}] = 4.0$ and $[\text{N}/\text{Fe}] = 2.3$, while the abundances of elements heavier than Mg are as low as Fe (Christlieb et al. 2002). Interestingly, this is not the only extremely metal poor (EMP) stars that have the large C/Fe and N/Fe ratios, but several other such stars have been discovered (Aoki et al. 2002). Therefore the reasonable explanation of the abundance pattern should explain other EMP stars as well. We show that the abundance pattern of C-rich EMP stars can be reasonably explained by the nucleosynthesis of 20 - 130 M_{\odot} supernovae with various explosion energies and the degree of mixing and fallback of the ejecta.

5.1. The Most Fe-Poor Star HE0107-5240

We consider a model that C-rich EMP stars are produced in the ejecta of (almost) metal-free supernova mixed with extremely metal-poor interstellar matter. We use Pop III pre-supernova progenitor models, simulate the supernova explosion and calculate detailed nucleosynthesis (Umeda & Nomoto 2003).

In Figure 5 (right) we show that the elemental abundances of one of our models are in good agreement with HE0107-5240, where the progenitor mass is $25 M_{\odot}$ and the explosion energy $E_{51} = 0.3$ (Umeda & Nomoto 2003).

In this model, explosive nucleosynthesis takes place behind the shock wave that is generated at $M_r = 1.8 M_{\odot}$ and propagates outward. The resultant abundance distribution is seen in Figure 5 (left), where M_r denotes the Lagrangian mass coordinate measured from the center of the pre-supernova model. The processed material is assumed to mix uniformly in the region from $M_r = 1.8 M_{\odot}$ and $6.0 M_{\odot}$. Such a large scale mixing was found to take place in SN1987A

and various explosion models (Hachisu et al. 1990). Almost all materials below $M_r = 6.0 M_\odot$ fall back to the central remnant and only a small fraction ($f = 2 \times 10^{-5}$) is ejected from this region. The ejected Fe mass is $8 \times 10^{-6} M_\odot$.

The CNO elements in the ejecta were produced by pre-collapse He shell burning in the He-layer, which contains $0.2 M_\odot$ ^{12}C . Mixing of H into the He shell-burning region produces $4 \times 10^{-4} M_\odot$ ^{14}N . On the other hand, only a small amount of heavier elements (Mg, Ca, and Fe-peak elements) are ejected and their abundance ratios are the average in the mixed region. The sub-solar ratios of $[\text{Ti}/\text{Fe}] = -0.4$ and $[\text{Ni}/\text{Fe}] = -0.4$ are the results of the relatively small explosion energy ($E_{51} = 0.3$). With this "mixing and fallback", the large C/Fe and C/Mg ratios observed in HE0107-5240 are well reproduced.

In this model, N/Fe appears to be underproduced. However, N can be produced inside the EMP stars through the C-N cycle, and brought up to the surface during the first dredge up stage while becoming a red-giant star (Boothroyd & Sackmann 1999).

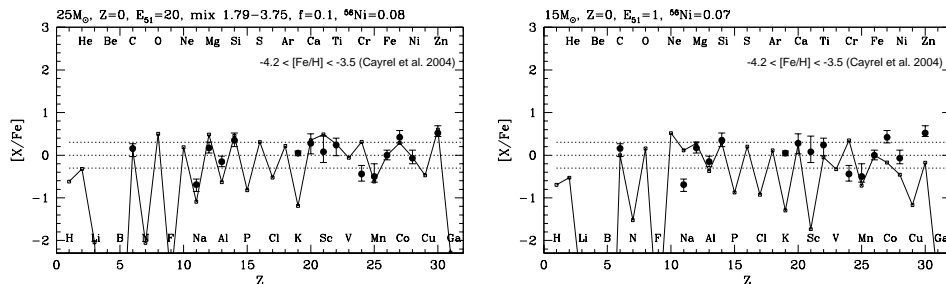


Figure 6. Averaged elemental abundances of stars with $[\text{Fe}/\text{H}] = -3.7$ (Cayrel et al. 2004) compared with the hypernova yield (left: $25 M_\odot$, $E_{51} = 20$), and the normal SN yield (right: $15 M_\odot$, $E_{51} = 1$).

5.2. EMP Stars from VLT Observations

The "mixing and fall back" process can reproduce the abundance pattern of the typical EMP stars without enhancement of C and N. Figure 6 shows that the averaged abundances of $[\text{Fe}/\text{H}] = -3.7$ stars in Cayrel et al. (2003) can be fitted well with the hypernova model of $25 M_\odot$ and $E_{51} = 20$ (left) but not with the normal SN model of $15 M_\odot$ and $E_{51} = 1$ (right) (Tominaga et al. 2005).

6. First Stars

It is of vital importance to identify the first generation stars in the Universe, i.e., totally metal-free, Pop III stars. The impact of the formation of Pop III stars on the evolution of the Universe depends on their typical masses.

6.1. High Mass vs. Low Mass

Recent numerical models have shown that, the first stars are as massive as $\sim 100 M_\odot$ (Abel et al. 2002). The formation of long-lived low mass Pop III stars may be inefficient because of slow cooling of metal free gas cloud, which is consistent with the failure of attempts to find Pop III stars.

Table 1. The results of the stability analysis for Pop III and Pop I stars. \bigcirc and \times represent that the star is stable and unstable, respectively. The e -folding time for the fundamental mode is shown after \times in units of 10^4yr (Nomoto et al. 2003).

mass (M_\odot)	80	100	120	150	180	300
Pop III	\bigcirc	\bigcirc	\bigcirc	\times (9.03)	\times (4.83)	\times (2.15)
Pop I	\bigcirc	\times (7.02)	\times (2.35)	\times (1.43)	\times (1.21)	\times (1.71)

If the most Fe deficient star, HE0107-5240, is a Pop III low mass star that has gained its metal from a companion star or interstellar matter (Yoshii 1981), would it mean that the above theoretical arguments are incorrect and that such low mass Pop III stars have not been discovered only because of the difficulty in the observations?

Based on the results in the earlier section, we propose that the first generation supernovae were the explosion of $\sim 20\text{--}130 M_\odot$ stars and some of them produced C-rich, Fe-poor ejecta. Then the low mass star with even $[\text{Fe}/\text{H}] < -5$ can form from the gases of mixture of such a supernova ejecta and the (almost) metal-free interstellar matter, because the gases can be efficiently cooled by enhanced C and O ($[\text{C}/\text{H}] \sim -1$).

6.2. Pair Instability SNe vs. Core Collapse SNe

In contrast to the core-collapse supernovae of $20\text{--}130 M_\odot$ stars, the observed abundance patterns cannot be explained by the explosions of more massive, $130 - 300 M_\odot$ stars. These stars undergo pair-instability supernovae (PISNe) and are disrupted completely (e.g., Umeda & Nomoto 2002; Heger & Woosley 2002), which cannot be consistent with the large C/Fe observed in HE0107-5240 and other C-rich EMP stars. The abundance ratios of iron-peak elements ($[\text{Zn}/\text{Fe}] < -0.8$ and $[\text{Co}/\text{Fe}] < -0.2$) in the PISN ejecta (Fig. 6; Umeda & Nomoto 2002; Heger & Woosley 2002) cannot explain the large Zn/Fe and Co/Fe in the typical EMP stars (McWilliam et al. 1995; Norris et al. 2001; Cayrel et al. 2003) and CS22949-037 either. Therefore the supernova progenitors that are responsible for the formation of EMP stars are most likely in the range of $M \sim 20 - 130 M_\odot$, but not more massive than $130 M_\odot$. This upper limit depends on the stability of massive stars as will be discussed below.

6.3. Stability and Mass Loss of Massive Pop III Stars

To determine the upper limit mass of the Zero Age Main Sequence (ZAMS), Nomoto et al. (2003) analyzed a linear non-adiabatic stability of massive ($80M_\odot - 300M_\odot$) Pop III stars using a radial pulsation code. Because CNO elements are absent during the early stage of their evolution, the CNO cycle does not operate and the star contracts until temperature rises sufficiently high for the 3α reaction to produce ^{12}C . We calculate that these stars have $X_{\text{CNO}} \sim 1.6 - 4.0 \times 10^{-10}$, and the central temperature $T_c \sim 1.4 \times 10^8 K$ on their ZAMS. We also examine the models of Pop I stars for comparison.

Table 1 shows the results for our analysis. The critical mass of ZAMS Pop III star is $128M_{\odot}$ while that of Pop I star is $94M_{\odot}$. This difference comes from very compact structures (with high T_c) of Pop III stars.

Stars more massive than the critical mass will undergo pulsation and mass loss. We note that the e -folding time of instability is much longer for Pop III stars than Pop I stars with the same mass, and thus the mass loss rate is much lower. These results are consistent with Ibrahim et al. (1981) and Baraffe et al. (2001). However, the absence of the indication of PISNe in EMP stars might imply that these massive stars above $130M_{\odot}$ undergo significant mass loss, thus evolving into Fe core-collapse rather than PISNe.

7. Type Ia/IIn Supernovae: SNe 2002ic, 1997cy, and 1999E

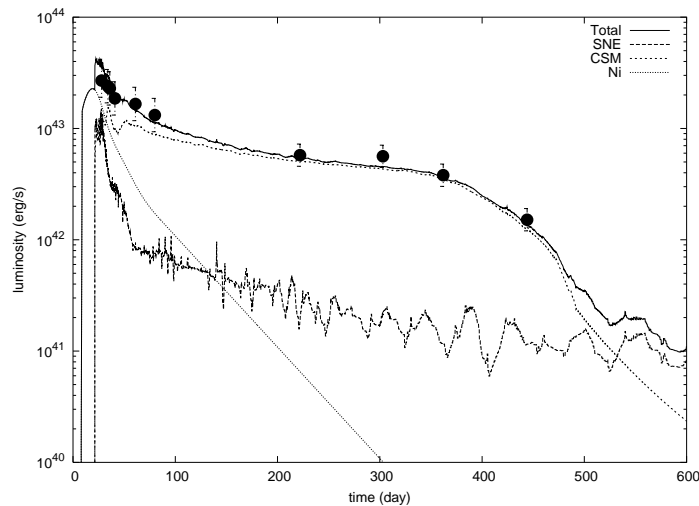


Figure 7. Model light curve (thick line: Nomoto et al. 2005) compared with the observation of SN 2002ic (filled circles; Deng et al. 2004).

SNe 1997cy and 1999E were initially classified as Type IIn because they showed $H\alpha$ emission. SN 2002ic would also have been so classified, had it not been discovered at an early epoch. SN 1997cy ($z = 0.063$) is among the most luminous SNe discovered so far ($M_V < -20.1$ about maximum light), and SN 1999E is also bright ($M_V < -19.5$). Both SNe 1997cy and 1999E have been suspected to be spatially and temporally related to a GRB (Germany et al. 2000; Rigon et al. 2003). However, both the classification and the associations with a GRB must now be seen as highly questionable in view of the fact that their replica, SN 2002ic, appears to have been a genuine SN Ia at an earlier phase (Hamuy et al. 2003; Deng et al. 2004).

Nomoto et al. (2005) calculated the interaction between the expanding ejecta and CSM (circumstellar matter). For the supernova ejecta, the carbon deflagration model W7 was used. After day ~ 350 , the light curve starts declining. To reproduce the declining part of the light curve, we add the outer CSM of $0.2 M_{\odot}$ where the density declines sharply as $n = 6$. This implies that the total mass of CSM is $\sim 1.3 M_{\odot}$.

References

- Abel, T., Bryan, G.L., & Norman, M.L. 2002, *Science*, 295, 93
- Aoki, W., Ryan, S.G., Beers, T.C., & Ando, H. 2002, *ApJ*, 567, 1166
- Audouze, J., & Silk, J. 1995, *ApJ*, 451, L49
- Baraffe, I., Heger, A., & Woosley, S.E. 2001, *ApJ*, 550, 890
- Boothroyd, A.I., & Sackmann, I.-J. 1999, *ApJ*, 510, 217
- Cayrel, R., et al. 2004, *A&A*, 416, 1117
- Christlieb, N., et al. 2002, *Nat*, 419, 904
- Christlieb, N., et al. 2004, *ApJ*, 603, 708
- Deng, J., Kawabata, K., Ohya, Y., Nomoto, K., et al. 2004, *ApJ*, 605, L37
- Galama, T., et al. 1998, *Nat*, 395, 670
- Germany, L. M., et al. 2000, *ApJ*, 533, 320
- Hachisu, I., Matsuda, T., Nomoto, K., & Shigeyama, T. 1990, *ApJ*, 358, L57
- Hamuy, M. 2003, *ApJ*, 582, 905
- Hamuy, M., et al. 2003, *Nat*, 424, 651
- Hatano, K., et al. 2001, *BAAS*, 198, 3902
- Heger, A., & Woosley, S.E. 2002, *ApJ*, 567, 532
- Hjorth, J., et al. 2003, *Nat*, 423, 847
- Ibrahim, A., Boury, A., & Noels, A. 1981, *A&A*, 103, 390
- Iwamoto, K., Mazzali, P.A., Nomoto, K., et al. 1998, *Nat*, 395, 672
- Iwamoto, K., Nakamura, T., Nomoto, K., et al. 2000, *ApJ*, 534, 660
- Knop, R., et al. 1999, *IAU Circ.* 7128
- Mazzali, P.A., Iwamoto, K., Nomoto, K. 2000, *ApJ*, 545, 407
- Mazzali, P.A., Deng, J., Maeda, K., Nomoto, K., et al. 2002, *ApJ*, 572, L61
- Mazzali, P.A., et al. 2003, *ApJ*, 599, L95
- McWilliam, A., Preston, G.W., Sneden, C., Searle, L. 1995, *AJ*, 109, 2757
- Nakamura, T., Umeda, H., Nomoto, K., Thielemann, F.-K., & Burrows, A. 1999, *ApJ*, 517, 193
- Nakamura, T., Mazzali, P.A., Nomoto, K., Iwamoto, K. 2001a, *ApJ*, 550, 991
- Nakamura, T., Umeda, H., Iwamoto, K., Nomoto, K., et al. 2001b, *ApJ*, 555, 880
- Nomoto, K., Mazzali, P.A., Nakamura, T., et al. 2001, in *Supernovae and Gamma Ray Bursts*, eds. M. Livio et al. (Cambridge Univ. Press), 144 (astro-ph/0003077)
- Nomoto, K., et al. 2003, in *IAU Symp 212, A Massive Star Odyssey, from Main Sequence to Supernova*, eds. V.D. Hucht, et al. (ASP), 395 (astro-ph/0209064)
- Nomoto, K., Suzuki, T., Deng, J., Uenishi, T., & Hachisu, I. 2005, 1604-2004 Supernovae as Cosmological Lighthouse, ed. L. Zampieri et al. (ASP), in press
- Norris, J.E., Ryan, S.G., & Beers, T.C. 2001, *ApJ*, 561, 1034
- Rigon, L., et al. 2003, *MNRAS* 340, 191
- Ryan, S.G., Norris, J.E., & Beers, T.C. 1996, *ApJ*, 471, 254
- Schneider, R., Ferrara, A., Natarajan, P., & Omukai, K. 2002, *ApJ*, 571, 30
- Shigeyama, T., & Tsujimoto, T. 1998, *ApJ*, 507, L135
- Sneden, C., Gratton, R.G., & Crocker, D.A. 1991, *A&A*, 246, 354
- Stanek, K.Z., et al. 2003, *ApJ*, 591, L17
- Tominaga, N., Umeda, H., Nomoto, K. 2005, in preparation
- Turatto, M., Mazzali, P.A., Young, T., Nomoto, K., et al. 1998, *ApJ*, 498, L129
- Umeda, H., & Nomoto, K. 2002, *ApJ*, 565, 385
- Umeda, H., Nomoto, K., Tsuru, T., & Matsumoto, H. 2002, *ApJ*, 578, 855
- Umeda, H., & Nomoto, K. 2003, *Nat*, 422, 871
- Umeda, H., & Nomoto, K. 2004, in preparation
- Umeda, H., & Nomoto, K. 2005, *ApJ*, 619, 427
- Woosley, S.E., Eastman, R.G., & Schmidt, B.P. 1999, *ApJ*, 516, 788
- Yoshii, Y. 1981, *A&A*, 97, 280
- Zampieri, L., et al. 2003, *MNRAS*, 338, 711